

RESONANT STRUCTURES IN HEAVY-ION REACTIONS

**MASTER**

by

S.J. Sanders, W. Henning, H. Ernst, D.F. Geesaman, C. Jachcinski,  
D.G. Kovar, M. Paul, and J.P. Schiffer

Prepared for  
Sixth Conference  
on the  
Applications of Accelerators in Research and Industry  
Denton, Texas  
November 3-5, 1980

**DISCLAIMER**

This book was prepared as an account of work sponsored by an agency of the United States Government. Neither the United States Government nor any agency thereof, nor any of their employees, makes any warranty, express or implied, or assumes any legal liability or responsibility for the accuracy, completeness, or usefulness of any information, apparatus, product or process disclosed, or represents that its use would not infringe privately owned rights. Reference herein to any specific commercial product, process, or service by trade name, trademark, manufacturer, or otherwise, does not necessarily constitute or imply its endorsement, recommendation, or favoring by the United States Government or any agency thereof. The views and opinions of authors expressed herein do not necessarily state or reflect those of the United States Government or any agency thereof.



**ARGONNE NATIONAL LABORATORY, ARGONNE, ILLINOIS**

**Operated under Contract W-31-109-Eng-38 for the  
U. S. DEPARTMENT OF ENERGY**

**DISTRIBUTION OF THIS DOCUMENT IS UNLIMITED** *JNS*

## RESONANT STRUCTURES IN HEAVY-ION REACTIONS

S. J. Sanders<sup>†</sup>, W. Henning, H. Ernst, D. F. Geesaman, C. Jachninski, D. G. Kovar, M. Paul<sup>††</sup>, and J. P. Schiffer  
Argonne National Laboratory  
Argonne, Illinois 60439

An investigation of heavy-ion resonance structures using the  $^{24}\text{Mg}(^{16}\text{O}, ^{12}\text{C})^{28}\text{Si}$  reaction is presented. The data are analyzed in the context of Breit-Wigner resonances added to a direct-reaction background.

### Introduction

The interactions of heavy-ion systems such as  $^{12}\text{C} + ^{28}\text{Si}$  and  $^{16}\text{O} + ^{24}\text{Mg}$  at energies ranging from the Coulomb barrier to several times the barrier height have been of considerable recent interest because of their apparent resonance character. With the large number of open reaction channels and the high density of states in the compound system with angular momenta near to that of the grazing value, it might be expected that any possible resonances in these interactions would have sufficiently large spreading width to be unobservable. This view was supported by the analysis of Cramer et al.<sup>1</sup> of forward angle elastic scattering data for the  $^{16}\text{O} + ^{28}\text{Si}$  system over the energy range  $33 \text{ MeV} \leq E_{\text{lab}} \leq 215.2 \text{ MeV}$ . Here an energy independent optical potential was found which could well reproduce the experimental data and which had the properties of being strongly absorbing and having a shallow real well depth. The first evidence that strong absorption does not give a complete picture was found by Braun-Munzinger et al.<sup>2</sup> who extended to  $\theta_{\text{lab}} = 180^\circ$  the elastic scattering measurements of  $^{16}\text{O} + ^{28}\text{Si}$  at  $E_{\text{lab}} = 55 \text{ MeV}$  and found that, rather than a relatively monotonic decrease of  $d\sigma/d\sigma_{\text{Ruth}}(\theta)$  to a value of  $10^{-6}$  as predicted by the strong absorption potential, the cross section ratio to Rutherford becomes highly oscillatory near  $\theta_{\text{c.m.}} = 70^\circ$  and reaches a value of  $d\sigma/d\sigma_{\text{Ruth}} \approx 10^{-2}$  at  $180^\circ$ . The far backward angle data are found to be characterized by a  $|P_\ell(\cos \theta)|^2$  angular dependence with angular momentum  $\ell$  near to that of the grazing value. Subsequent excitation functions measured by Barrette et al.<sup>3</sup> for the  $180^\circ$  elastic and inelastic scattering of  $^{16}\text{O} + ^{28}\text{Si}$  and  $^{12}\text{C} + ^{28}\text{Si}$  showed dramatic resonance features regularly spaced in energy and of widths  $\Gamma_{\text{tot}} \sim 1-3 \text{ MeV}$ .

In this paper a series of measurements on the  $^{24}\text{Mg}(^{16}\text{O}, ^{12}\text{C})^{28}\text{Si}$  reaction are presented and discussed within a resonance framework. A transfer reaction has the advantage for studying heavy-ion resonances that, as compared to elastic and inelastic scattering, there is substantially less non-resonant background. We chose to investigate this particular reaction for a number of reasons: as mentioned, the  $^{12}\text{C} + ^{28}\text{Si}$  channel is one in which resonance features have been observed; the transfer reaction to the  $^{28}\text{Si}$  ground- and first-excited states<sup>4,5</sup> and a number of other low-lying excited states<sup>7</sup> have been investigated at forward angles and found to be well modeled by DWBA calculations and finally, some evidence<sup>6</sup> for resonance structures have been observed in the backward angle inelastic scattering of  $^{16}\text{O}$  to the  $2^+$  first-excited state of  $^{24}\text{Mg}$  and in the  $^{24}\text{Mg}(^{16}\text{O}, ^{12}\text{C})^{28}\text{Si}$  reaction to the first  $0^+$  and  $2^+$  states of  $^{28}\text{Si}$ .

### Experimental Methods

The data were obtained using the Argonne FN tandem-Van de Graaff accelerator, the Brookhaven MP-7 tandem Van de Graaff accelerator, and the Argonne FN tandem-LINAC booster facility. Forward angle measurements were taken at

Argonne where the reaction products were momentum analyzed in an Enge split-pole magnetic spectrograph and detected in an ionization-chamber, focal-plane detector. For measurements at and near to  $0^\circ$ , an Au foil was placed in front of the detector to stop the  $^{16}\text{O}$  beam. The particles passing into the counter yielded  $\Delta E$ -E signals for Z identification. Since a spectrograph was not available at the LINAC booster facility at Argonne, for these measurements a  $\Delta E$ -E telescope with Si(SB) detectors was used to determine the energy and Z of the reaction products. All of the backward-angle data ( $\theta_{\text{c.m.}} > 120^\circ$ ) were obtained at Brookhaven by studying the kinematically reversed reactions with  $^{24}\text{Mg}$  as the projectile and the lighter outgoing particles detected at forward angles in the BNL-QDDD magnetic spectrograph. A double-wire proportional counter was used for position and  $\Delta E$ -E information, and, again, for measurements near  $\theta_{\text{lab}} = 0^\circ$  the detector was shielded from the primary  $^{24}\text{Mg}$  beam by the use of absorber foils. The beam energy spread resulting from the target thicknesses was typically 300-500 keV for both the forward- and backward-angle measurement. Further details of the experimental techniques and the normalization procedures can be found in references 7-10.

### Results and Discussion

In Fig. 1 we show the elastic scattering of  $^{16}\text{O} + ^{24}\text{Mg}$  at  $E_{\text{c.m.}} = 27.8 \text{ MeV}$  over the angular range  $80^\circ < \theta_{\text{c.m.}} < 180^\circ$ . The cross section ratio  $d\sigma/d\sigma_{\text{Ruth}}$  is found to drop to 0.1% before rising at backward angles to 10% at  $180^\circ$ . The far backward-angle data is found to be highly oscillatory with a spacing of the cross section maxima roughly that for a  $|P_\ell(\cos \theta)|^2$  angular dependence with  $\ell = 20 \pm 1$ . This backward angle rise in the  $^{16}\text{O} + ^{24}\text{Mg}$  elastic scattering data is similar to that found in  $^{12}\text{C} + ^{28}\text{Si}$  scattering<sup>3</sup> and, hence, in both the entrance- and exit-channel elastic scattering for the  $^{24}\text{Mg}(^{16}\text{O}, ^{12}\text{C})^{28}\text{Si}$  reaction are found similarly enhanced backward-angle yields above that expected from a strong absorption model.

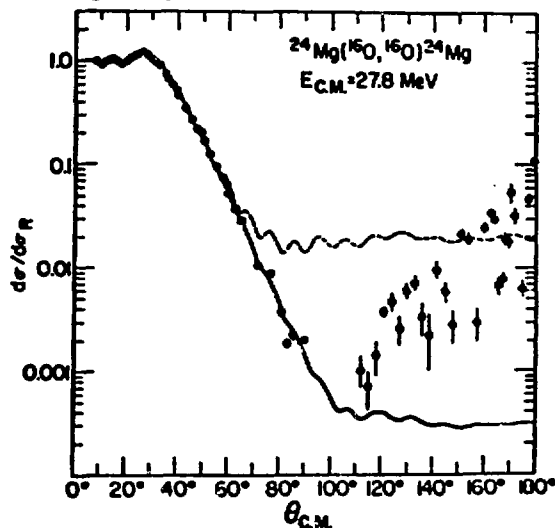


Figure 1. Elastic scattering of  $^{16}\text{O} + ^{24}\text{Mg}$ .

The two curves shown in Fig. 1 are the elastic scattering predictions of optical model potentials which are used in DWBA calculations for the transfer reaction. The dashed curve is derived using the potential ANL1 (see Table 1) of Erskine et al.<sup>4</sup> This potential, which successfully reproduces the general behavior of the transfer reaction data at forward angles ( $\theta_{c.m.} < 50^\circ$ ) over the energy range  $26 \text{ MeV} < E_{c.m.} < 33 \text{ MeV}$  for both the ground-state<sup>4, 7, 9</sup> and several excited-state transitions,<sup>10</sup> is employed in the Breit-Wigner resonance analysis discussed later in this paper. The solid curve in Fig. 1 shows the elastic scattering calculated using a potential which was fitted to forward-angle elastic-scattering data at  $E_{c.m.} = 27.8 \text{ MeV}$  and  $36.2 \text{ MeV}$  by fixing the well depths at the ANL1 values and then varying the geometric parameters. These fitted parameters are listed in Table 1 as ANL3. Applying the ANL3 parameters to the  $^{24}\text{Mg}(^{16}\text{O}, ^{12}\text{C})^{28}\text{Si}(g.s.)$  transfer reaction calculations, we have found substantially poorer agreement with experiment at  $27.8 \text{ MeV}$ , whereas at  $36.2 \text{ MeV}$  the transfer predictions of the two potentials are similar.

Angular distributions for the  $^{24}\text{Mg}(^{16}\text{O}, ^{12}\text{C})^{28}\text{Si}(g.s.)$  reaction at  $E_{c.m.} = 27.8 \text{ MeV}$  and  $36.2 \text{ MeV}$  are shown in Fig. 2 for  $0^\circ \leq \theta_{c.m.} \leq 180^\circ$ . As was found for the elastic channels, the back angle yields in the transfer reaction are found to be strongly enhanced over that expected for a direct (non-resonant) process. Typical  $180^\circ$  yields predicted by DWBA calculations are one to several orders of magnitude less than the observed yields. Further, the backward angle yields at both energies are well characterized by a  $|P_\ell(\cos \theta)|^2$  angular dependence with  $\ell = 20 \pm 1$  at  $E_{c.m.} = 27.8 \text{ MeV}$  and  $\ell = 26 \pm 1$  at  $E_{c.m.} = 36.2 \text{ MeV}$ . We note that, within our uncertainties, the backward angle data in the  $^{16}\text{O} + ^{24}\text{Mg}$  channel and the transfer data appear to be characterized by the same dominant angular momentum at  $E_{c.m.} = 27.8 \text{ MeV}$ .

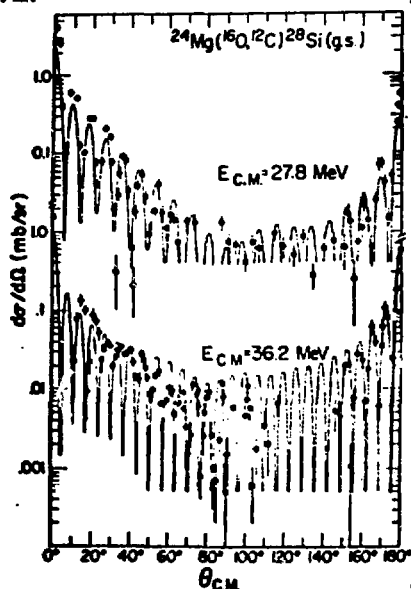


Figure 2. Transfer reaction data at  $E_{c.m.} = 27.8 \text{ MeV}$  and  $36.2 \text{ MeV}$ . The curves, discussed in the text, are DWBA calculations where additional resonance strength is added to a single partial wave ( $\ell = 20$  at  $E_{c.m.} = 27.8 \text{ MeV}$  and  $\ell = 27$  at  $E_{c.m.} = 36.2 \text{ MeV}$ ).

How well these  $^{24}\text{Mg}(^{16}\text{O}, ^{12}\text{C})^{28}\text{Si}(g.s.)$  angular distributions can be understood in a resonance picture is

seen by decomposing the reaction amplitude for the resonant partial wave into a sum of a direct part, which varies slowly with energy, and a resonant part. The cross section for a reaction involving spin-zero particles in both the incoming and outgoing channels is then given by

$$d\sigma/d\Omega = \left| \sum_{\ell} \frac{1}{2ik_{in}} (2\ell + 1) f_{\ell}^{tot} P_{\ell}(\cos \theta) \right|^2 \quad (1)$$

where

$$f_{\ell}^{tot} = f_{\ell}^{res} + f_{\ell}^{dir} \quad (2)$$

The resonance term in eq. 2 vanishes for  $\ell \neq \ell_{res}$ , and the direct part of the amplitude  $f_{\ell}^{dir}$  can be approximated by a calculated distorted wave amplitude  $f_{\ell}^{DWBA}$ . Assuming an optical potential to be used in both channels of the DWBA calculation, this is a three parameter fit of the DWBA normalization and the complex number  $f_{\ell}^{res}$ . The DWBA normalization is most sensitive to the forward angle data, whereas the magnitude  $|f_{\ell}^{res}|$  is essentially fixed by the backward angle data. The results of this analysis applied to the data are shown as the curves in Fig. 2.

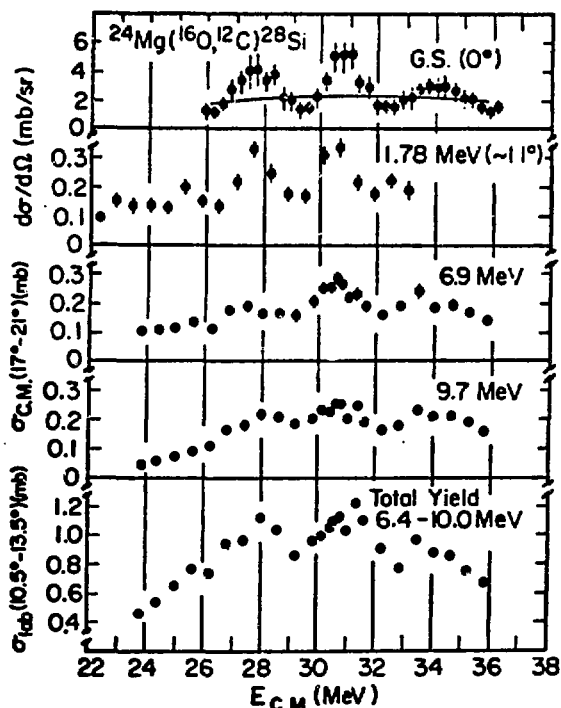


Figure 3. Forward-angle excitation functions for a number of the  $^{24}\text{Mg}(^{16}\text{O}, ^{12}\text{C})^{28}\text{Si}^*$  reaction channels.

The relatively large magnitude of the resonance term  $f_{\ell}^{res}$  found at  $E_{c.m.} = 27.8 \text{ MeV}$  and  $36.2 \text{ MeV}$  with respect to the non-resonant background for the transfer reaction (as indicated by  $\sigma(180^\circ)/\sigma(0^\circ) \sim 10-30\%$ ), suggests that resonance effects should be observable at forward angles with the transfer reaction. In Fig. 3 we show excitation functions<sup>7, 9, 10</sup> of forward angle yields for several of the well resolved states in  $^{28}\text{Si}$ : the ground state ( $J^\pi = 0^+$ ), the  $1.78 \text{ MeV}$  level ( $J^\pi = 2^+$ ), a  $6.9 \text{ MeV}$  doublet ( $J^\pi = 3^- + 4^+$ ), and the  $9.7 \text{ MeV}$  level ( $J^\pi = 5^-$ ). The excitation functions of all four levels show similar, and strongly correlated, resonance features. These structures are totally unexpected from DWBA calculations. For the ground state transition the predicted direct (DWBA) behavior using the

ANL1 optical potential in both entrance and exit channels is shown. Also shown in Fig. 3 is the integrated yield for  $6.4 \text{ MeV} < E_x(\text{Si}) < 10 \text{ MeV}$ . The peak-to-valley ratios in this summed yield plot are greater than can be accounted for with just summing the 6.9 MeV and 9.7 MeV levels. Angular distributions for  $10^\circ < \theta_{\text{c.m.}} < 50^\circ$  of the transitions to the 6.9 MeV and 9.7 MeV levels are found<sup>10</sup> to be relatively featureless with a monotonic decrease in cross section as a function of angle. These angular distributions are well fitted by DWBA calculations using the ANL1 potential.

The excitation functions shown in Fig. 3 offer the strongest evidence yet that these cross sections are influenced by true resonances of the compound system. It is unlikely that any dynamic (as opposed to structural) effects could result in such similar behavior for the different channels. Measurements to test whether  $^{24}\text{Mg}$  excited states will show similar correlated features by studying the  $^{28}\text{Si}(^{12}\text{C}, ^{16}\text{O})^{24}\text{Mg}^*$  reactions are in progress.

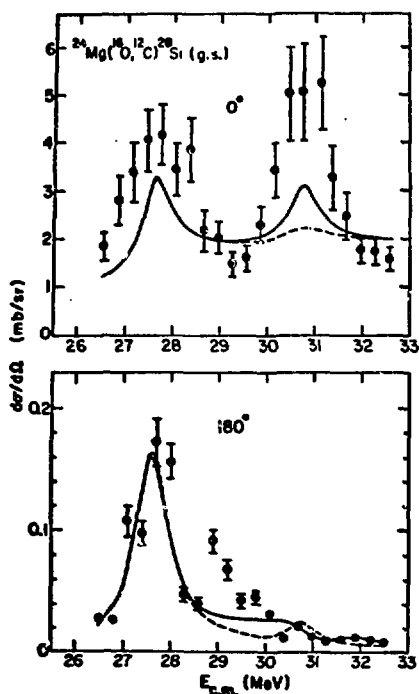


Figure 4. Excitation functions for the  $^{24}\text{Mg}(^{16}\text{O}, ^{12}\text{C})^{28}\text{Si}$  (g.s.) reaction at  $\theta_{\text{c.m.}} = 0^\circ$  and  $180^\circ$ .

Returning to the ground state transition, a possible problem for obtaining a consistent resonant interpretation is the lack of any strong overall correlations between the forward and backward angle transfer data. This is shown in Fig. 4 where we plot the  $0^\circ$  and  $180^\circ$  excitation functions for the  $^{24}\text{Mg}(^{16}\text{O}, ^{12}\text{C})^{28}\text{Si}$  (g.s.) reaction. At  $E_{\text{c.m.}} = 27.8 \text{ MeV}$  there are strong peaks in both the  $0^\circ$  and  $180^\circ$  excitation functions, whereas at  $E_{\text{c.m.}} = 30.8 \text{ MeV}$  there is a peak at forward angles -- but not at backward angles. Although not shown, at  $E_{\text{c.m.}} = 36.2 \text{ MeV}$  there is a strong maximum in the  $180^\circ$  yield, and a dip in the  $0^\circ$  yield (see ref. 9). For understanding these behaviors in a resonance picture, we have attempted<sup>9</sup> to parametrize the energy dependence of  $f_{\ell}^{\text{res}}$  by a Breit-Wigner form:

$$f_{\ell}^{\text{res}} = f \exp[i(\varphi_{\text{nucl}} + \sigma_{\text{in}} + \sigma_{\text{out}} + \varphi)] \times \frac{\sqrt{\Gamma_{\text{in}} \Gamma_{\text{out}}}}{E_0 - E - i\Gamma/2} \quad (3)$$

where the overall phases include the DWBA nuclear phase  $\varphi_{\text{nucl}}$  and the incoming and outgoing Coulomb phases  $\sigma_{\text{in}}$  and  $\sigma_{\text{out}}$ . The additional phase  $\varphi$  was kept fixed over the full energy range and was treated as an adjustable parameter. The incoming and outgoing partial widths  $\Gamma_{\text{in}}$  and  $\Gamma_{\text{out}}$  are expressed in terms of energy independent reduced widths by factoring out the Coulomb and centrifugal-barrier penetrabilities:

$$\Gamma_{\text{in(out)}}^2 = 2P_{\ell}^{\text{in(out)}} \gamma_{\text{in(out)}}^2 \quad (4)$$

where the penetrability factor can be expressed in terms of regular and irregular Coulomb wavefunctions as

$$P_{\ell} = \frac{kR}{F_{\ell}^2 + G_{\ell}^2} \quad (5)$$

For the present analysis the radius parameter  $R$  was taken as  $1.6 \times (A_1^{1/3} + A_2^{1/3}) \text{ fm}$ . The DWBA amplitudes  $f_{\ell}^{\text{DWBA}}$  were calculated using the ANL1 potential.

In Fig. 4 and 5 we show the result of such a Breit-Wigner fit to the transfer data with  $26.3 \text{ MeV} \leq E_{\text{c.m.}} \leq 32.4 \text{ MeV}$  (in addition to the data shown, this fit includes backward angle data at 27.8 and 30.8 MeV, as well as  $90^\circ$  cross sections at 10 energies spanning this range). At least two resonances must be included to reproduce the  $0^\circ$  excitation function in this energy range. For this analysis, we have assumed an  $\ell = 20$  resonance at  $E_{\text{c.m.}} = 27.8 \text{ MeV}$ . The energy independent analysis of the full angular distribution at 27.8 MeV, as discussed, indicates an  $\ell$  assignment of between 19 and 21. The  $\theta_{\text{c.m.}} = 90^\circ$  excitation function<sup>9</sup> for the reaction, however, has a strong maximum at 27.8 MeV, which indicates an even partial wave enhancement. For the second strong maximum found in the  $0^\circ$  yield near 30.8 MeV, there is a minimum in the  $90^\circ$  excitation function -- which is consistent with an odd  $\ell$  assignment -- but there is also a relative minimum in the  $180^\circ$  excitation function. These features can only be understood by the interference of at least two partial waves, one even and one odd. This is clearly seen in Fig. 4 where we plot the results of our Breit-Wigner analysis assuming  $\ell = 20 + 22$  assignments (dashed curve) and  $\ell = 20 + 23$  assignments (solid curve). Only with the  $\ell = 20 + 23$  assignments do we obtain sufficient interference from the lower energy resonance ( $\ell = 20$  near  $E_{\text{c.m.}} = 27.8 \text{ MeV}$ ) near the higher energy resonance ( $\ell = 23$  near  $E_{\text{c.m.}} = 30.8 \text{ MeV}$ ) to have a maximum in the  $0^\circ$  yield and a minimum in the  $180^\circ$  yield. The results of the two resonance fit with  $\ell = 20 + 23$  are also shown as compared with forward angle yields in Fig. 5. Both the full widths ( $\sim 800 \text{ keV}$ ) and reduced widths ( $\gamma_{\text{in}} \times \gamma_{\text{out}} \sim 0.8 \text{ keV}$ ) for the two resonances are comparable.

One question left unanswered concerns the extended energy dependence of the resonance structures. Naively, one might expect that as the center-of-mass energy increases the number of open channels, and, hence, the absorptiveness of the two-body optical potential would increase (ignoring the surface nature of the interact). With increased absorptiveness the resonance spreading width should also increase, resulting in broadened structures in the excitation functions. To test this, we have extended our  $0^\circ$  excitation function for the  $^{24}\text{Mg}(^{16}\text{O}, ^{12}\text{C})^{28}\text{Si}$  reaction to  $E_{\text{c.m.}} = 53 \text{ MeV}$  using the Argonne superconducting LINAC booster. These results are shown in Fig. 6. We find that the resonance structures do persist to the highest energies measured with no evidence for an increasing width. The structures are also found to be remarkably evenly spaced over the full energy range

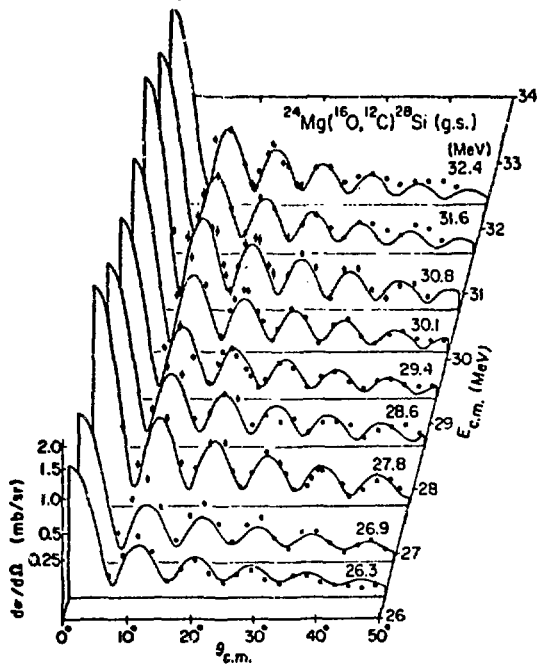


Figure 5. Angular distributions at a number of energies over the range of the two-resonance fit discussed in the text.

$26 \text{ MeV} \leq E_{c.m.} \leq 53 \text{ MeV}$ , such as would be expected for a harmonic potential. From our resonance analysis, however, this equal spacing must be viewed as a coincidence -- although we found at 27.8 and 30.8 MeV that the resonance amplitude constructively interfered with the direct background, at 36.2 MeV the interference is destructive resulting in a relative minimum for the  $0^0$  yield excitation function.

### Conclusions

Heavy-ion transfer reaction measurements, in companionship with elastic and inelastic scattering measurements, offer sensitive probes for unexpected, and apparently simple nuclear structures at very high temperatures and angular momenta. We have shown that the general features of the  $^{24}\text{Mg}(^{16}\text{O}, ^{12}\text{C})^{28}\text{Si}(\text{g.s.})$  excitation functions at both forward and backward angles can be understood in a consistent manner by the presence of a few resonances in the compound system. For the structures presented in this paper we are well above ( $\sim 15 \text{ MeV}$ ) the lowest energy level in the compound nucleus for the measured spin, and in a region where the density of states is on the order of  $10^4$  to  $10^5$  levels/MeV. This contrasts markedly with similar structures observed in the scattering of lighter systems such as  $^{12}\text{C} + ^{12}\text{C}$ .<sup>12</sup> Although only speculations can be offered on the origin of these structures -- perhaps in real nuclear systems there are structures related to the shape resonances of the elastic channels -- any discussion of these structures must rest on a careful determination of their properties.

This work was performed under the auspices of the U. S. Department of Energy.

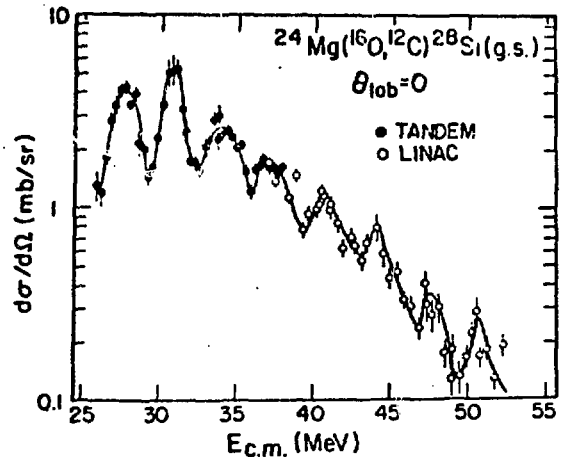


Figure 6. The excitation function for the  $^{24}\text{Mg}(^{16}\text{O}, ^{12}\text{C})^{28}\text{Si}(\text{g.s.})$  reaction. The curve is to guide the eye.

Table 1. Optical Model Potentials

	V (MeV)	$r_0$ (fm)	a (fm)	W (MeV)	$r_{i0}$ (fm)	$a_i$ (fm)	$r_{co}$ (fm)
ANL1 <sup>a</sup> )	37	1.35	0.404	78	1.290	0.174	1.2
ANL3	37	1.309	0.525	78	1.265	0.334	1.2

### References

- † Present address: Physics Dept., Yale Univ., New Haven, CT 06511.
- †† Present address: Racah Inst. of Physics, The Hebrew Univ. of Jerusalem, Israel.
1. J. Cramer, et al., Phys. Rev. C **14** (1976) 2158.
2. P. Braun-Munzinger, et al., Phys. Rev. Lett. **38** (1977) 944.
3. J. Barrette, et al., Phys. Rev. Lett. **40** (1978) 445.
4. J.R. Erskine, et al., Phys. Rev. Lett. **34** (1975) 680.
5. J.C. Peng, et al., Nucl. Phys. A**264** (1976) 312.
6. P. Chevallier, et al., Proceedings of the International Conf. on Nucl. Structure, Tokyo, 1977 (Organizing Comm., Tokyo, 1977).
7. M. Paul, et al., Phys. Rev. Lett. **40** (1978) 1310.
8. M. Paul, et al., Phys. Rev. C **21** (1980) 1802.
9. S.J. Sanders, et al., Phys. Rev. C **21** (1980) 1810.
10. S.J. Sanders, et al., Phys. Rev. C (1980) to be published.
11. Code PTOLEMY, M.H. Macfarlane and S.C. Pieper, Argonne Nat'l Laboratory Informal Report No. ANL-76-11 Rev. 1, 1978 (unpublished).
12. D.L. Hanson, et al., Phys. Rev. C **9** (1974) 1760.